

Article

Failure Propagation Controlling for Frangible Composite Canister Design

Aniello Smarrazzo ¹, Michele Guida ^{1,*} , Francesco Marulo ¹ , Massimo Coppola ² and Raffaele Moliterno ²¹ Department of Industrial Engineering, University of Naples Federico II, Via Claudio, 21, 80125 Naples, Italy² MBDA ITALIA, Via Carlo Calosi, 1, Bacoli, 80070 Naples, Italy

* Correspondence: michele.guida@unina.it

Abstract: The complexity in predicting the damage initiation and failure propagation controlling in composite structures is challenging. The focus of this paper is to design a potential component for new ship gunnells to make the composite canister affordable in structural applications by using a damage tolerant design approach. The design of a new tailgate configuration was investigated, taking into account the correct fragmentation of the structure to ensure a clear ejection while reducing the weight of the panels by exploiting the properties of the composite material. The complex geometry of the tailgate, the high impulse load, the energy transferred to the tailgate during missile impact, and how to safely break large panel flaps are elements that characterize the sizing of the composite component to meet the stringent ejection requirements in the life cycle of a missile during takeoff. The numerical simulations were performed using the LS/Dyna code and its explicit formulation was contemplated to take into account the geometrical, contact, and material non linearities.

Keywords: controlled rupture; progressive failure; composite material; FE analysis; nonlinear



Citation: Smarrazzo, A.; Guida, M.; Marulo, F.; Coppola, M.; Moliterno, R. Failure Propagation Controlling for Frangible Composite Canister Design. *Appl. Sci.* **2022**, *12*, 12220. <https://doi.org/10.3390/app122312220>

Academic Editors: Aniello Riccio and Angela Russo

Received: 19 October 2022

Accepted: 24 November 2022

Published: 29 November 2022

Publisher's Note: MDPI stays neutral with regard to jurisdictional claims in published maps and institutional affiliations.



Copyright: © 2022 by the authors. Licensee MDPI, Basel, Switzerland. This article is an open access article distributed under the terms and conditions of the Creative Commons Attribution (CC BY) license (<https://creativecommons.org/licenses/by/4.0/>).

1. Introduction

A canister cover protects a missile from foreign object intrusion, shock, and weather effects such as rain and waves, and facilitates smooth ejection during missile launch. The first covers were represented from rigid doors [1] or covers that are ruptured by explosive means prior to missile launch [2].

Doane [3] introduced a breakable cover using glass/epoxy laminae so that with the passage of the missile the cover would break, however, this solution didn't prevent the surface of the missile from being damaged during the launch, while Choi et al. [4] numerically estimated the degradation of launch performance caused by the remnants of a missile canister cover with a sabot interface. An alternative solution aimed at ensuring the integrity of the missile during launch has been proposed by Wu et al. [4]; this solution was validated by experimental tests and it consisted of a number of laminated composite canister covers fabricated and subjected to static burst pressure testing.

Recently, the preferred canister cover is usually the rupture-type, which is easily manufactured and provides excellent handling, even though it could potentially compromise the adjacent structure if the missile canister cover does not break during launch.

An innovative concept for a canister, consisting of a single carbon fiber composite laminate, is investigated, and by varying the geometric configuration, it is possible to optimize the fracture path and the contact force, as done with scaled panels subject to impact loads on the composite material [5,6]. To trigger the fracture, some areas without fibers called carvings were formed to delineate triangular fragments, which were named petals. The approach used in this work is based on the Chang-Chang failure criterion [7], which was used for damage initiation and failure propagation controlling of the canister cover, the first-ply failure prediction of laminated composite plates was verified in several work comparing the experimental results [8,9]. Davies et al. in the work [10] applied the Chang-Chang criterion in analyzing the quasi-isotropic carbon/epoxy composite laminates under

low-velocity impact, conversely Ghasemnejad [11] used it for high velocities. Meanwhile, a failure analysis of a frangible cover was studied based on transient dynamics via the finite element method in comparison with the experimental results [5].

The aim is to design a suitable tailgate shape that improves reliability and ensures the safe launch and good protection during the life of the missile. The goal of this work is to develop a scientific and methodological approach to the study of the controlled fracture structure for the design and optimization of the missile tailgate.

The state of the art with regard to the sea canister consists of the enclosure that contains the missile on the deck of the ship and is the only protection from external impact. The canister is usually made of metal, while the cover is made of polymer or ceramic materials, as shown in Figure 1. To prevent damage to the missile tip, in some cases a sabot is inserted between the missile and the cover to reduce the impact force.



Figure 1. Overview of a similar canister for a Harpoon missile [4].

Usually, the tailgate type varies according to size, velocity envelopes and environment. Small size missile covers consist of flexible or breakable tabs, while medium and large size missile tailgates have a mechanical opening or are the rupture-type which have a programmed break. Common configurations have a four-pavilion dome, and the missile is placed on a trolley in the canister as shown in Figure 2 below.



Figure 2. Aspid 30 system (left) and Aster system (right).

The Marte ER in Figure 3 is one of the most successful missiles produced by MBDA, and has a four-pavilion configuration with an internal stiffener at the tip which puts it in contact with the missile tip and the tailgate top. The stiffeners and the tailgate design provide a proper tailgate fragmentation, reducing contact force and accelerating the petals, as shown in Figure 4.

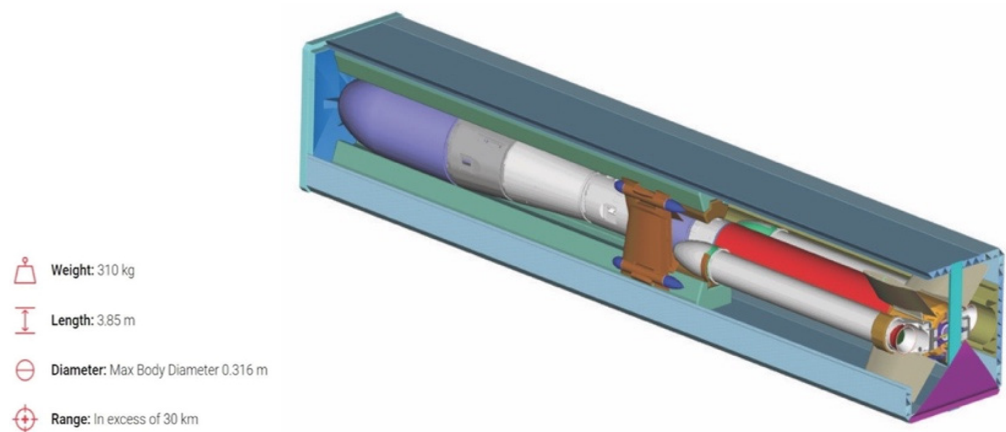


Figure 3. Marte ER System and Missile CAD.



Figure 4. Marte ER missile ejection.

2. Best Practices for the Design of Rupture-Controlled Structures

The expected conditions used for the canister design verification are presented in the diagram reported in Figure 5. Here all possible processes are discussed, and relevant loading processes are identified. As a result, mechanical loads are then processed into a series of fracture load, strength and toughness analyses, and are finally summarized in this research study. The canister must be designed and handled so that the operating conditions postulated during encapsulation, storage, transport and deposition do not cause any damage or change in properties that could affect the ability of the container to isolate its contents from the environment and external for the analysis period, in addition to the normal operating loads when the break occurs to allow the missile to escape.

The first phase requires the creation of a FEM model that describes the product and can simulate the behavior of the structure, as depicted in Figure 5. The validated computational model of the structure has to predict the failure initiation location and load, thanks to the failure theories and the progressive failure patterns, sizes, and final failure loads.

The goal is to obtain a strategic design of the structure by establishing guidelines and design criteria. For this purpose, it is very important to determine the probable impact conditions, considering impact velocities and angular velocities. The following conceptual map presents a possible workflow for designing a structure that achieves all objectives. Once the impact scenario and boundary conditions are determined, the impact force is

estimated, and the allowable motions are defined, as shown in Figure 6. These represent the spatial structure design criteria and the hardness design criteria. If both requirements are met, a structure can be idealized in the first attempt, but the weight is still a constraint. By iterating the procedure, the structure will meet all of the targets.

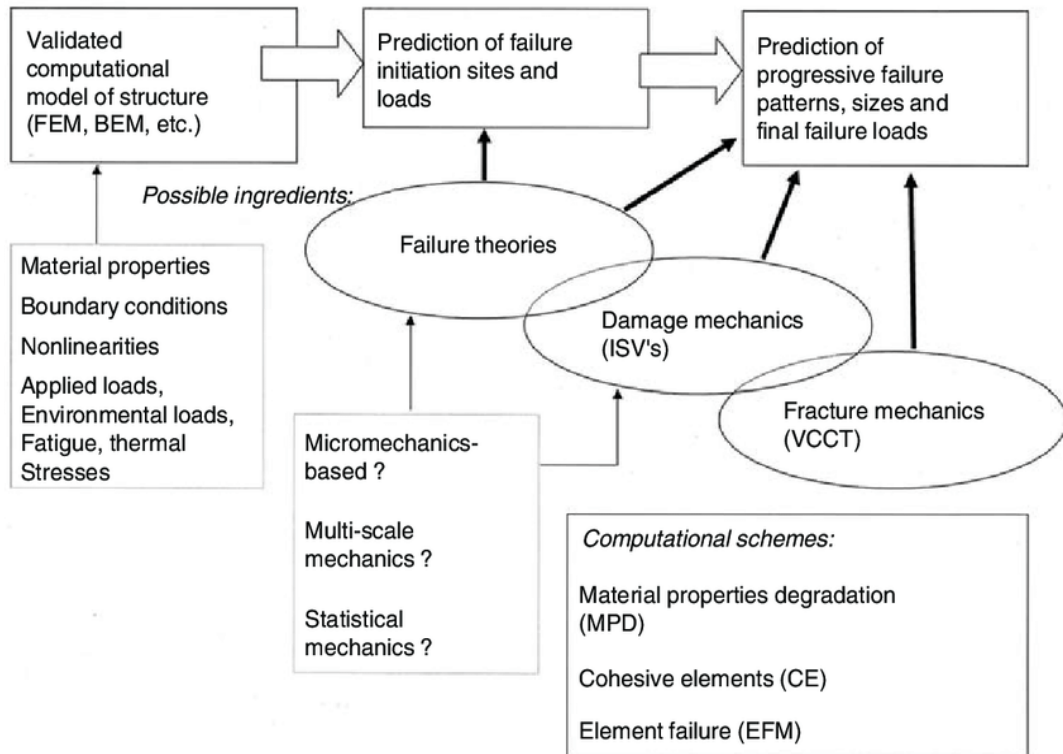


Figure 5. Modelling impact scenario.

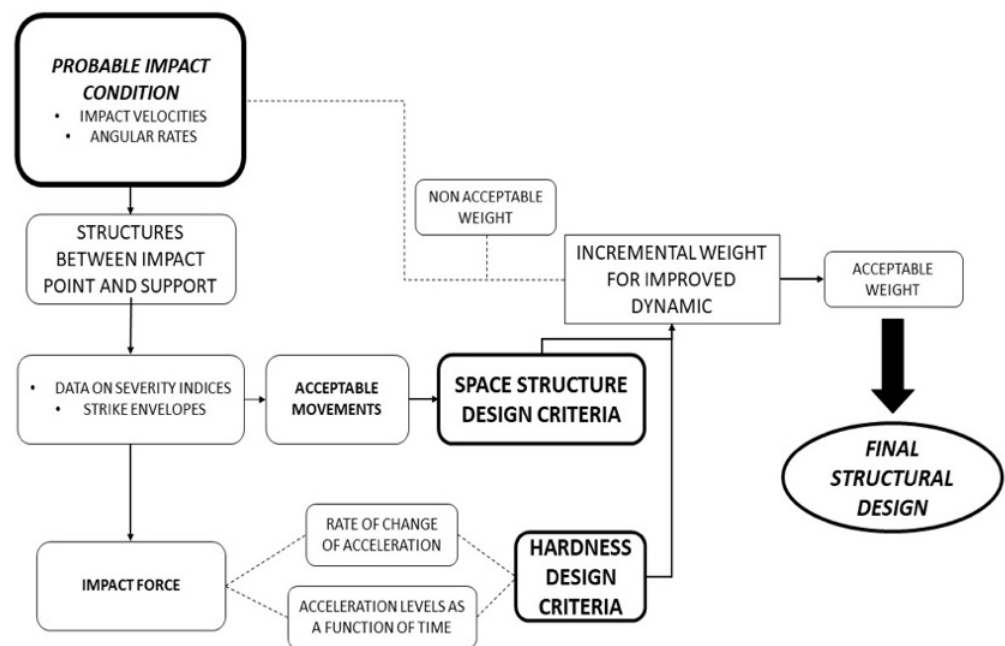


Figure 6. Concept Map: Design of Rupture-Controlled Structures Flow Chart.

Failure Criteria

Failure criteria for composite materials are often classified into two groups:

- non-interactive failure criteria (associated with failure modes) or the limit criterion is defined as one having no interactions between the stress or strain components. In detail, it means that the failure criterion evaluates failure based on a single stress component and does not take into consideration a multi-axial stress state in a structure and how the combination of different stress components affects the failure initiation in a composite ply.
- interactive failure criteria (associated with failure modes and not) involve interactions between stress or strain components. The objective of this approach is to allow for the fact that failure loads when a multi-axial stress state exists in the material may well differ from those when only a uniaxial stress is acting. Interactive failure criteria are mathematical in their formulation. Interactive failure criteria fall into three categories: polynomial theories, direct mode determining theories, and strain energy theories. The strain energy theories are based on local strain energy levels determined during a nonlinear analysis.

The LS-DYNA software has within its library several material models (constitutive law and failure criteria) specifically designed for composite materials when they are simulated, exploiting a macro homogenous approach. In this case, the fibre and matrix are not reproduced separately but in a unique assembly [12]. Therefore, it is fundamental to have reliable criteria that allow mimicking both the constitutive behaviour and the failure mechanisms. From literature, good results were obtained using MAT_54, therefore this material model was selected and used in the present activity [13].

MAT54 is designed to specifically simulate orthotropic materials with greatly differing properties in the longitudinal and transverse directions, such as unidirectional (UD) composite laminates and not fabric materials [14]. For this reason, it implements a matrix-specific failure criterion in the transverse direction that would not be appropriate to evaluate a fiber-dominated material. Nevertheless, MAT54 has been used to simulate fabric composite structures in crash simulations [15,16]. The LS-DYNA Keyword User's Manual entry for MAT54 provides little information other than defining the failure criterion and the degradation scheme, as reported in the Table 1.

Table 1. Material properties.

Property	Symbol
density	ρ
Modulus in 1-direction	E_1
Modulus in 2-direction	E_2
Shear modulus	G_{12}
Major Poisson's ratio	ν_{12}
Minor Poisson's ratio	ν_{21}
Strength in 1-direction, tension	F_1^{tu}
Strength in 2-direction, tension	F_2^{tu}
Strength in 1-direction, compression	F_1^{cu}
Strength in 2-direction, compression	F_2^{cu}
Shear strength	F_{12}^{su}

MAT54—MAT_ENHANCED_COMPOSITE_DAMAGE was developed from MAT22—COMPOSITE_DAMAGE. It is based on the Chang-Chang failure criteria for the damage onset and it has a linear elastic behaviour before reaching the materials strength [8]. As a consequence, before the damage occurs, the model has a linear elastic behaviour. When the maximum stress is reached, damage initiates. Basically, this model assumes three different in-plane failure modes: matrix cracking, fibre-matrix shearing, and fibre breakage. In addition to this, for material model 54 a compressive failure is considered. Below,

the failure criteria used to predict in-plane failure for the corresponding failure modes are reported:

Tensile fibre mode:

$$\sigma_{11} > 0 \text{ then } e_f^2 = \left(\frac{\sigma_{11}}{X_f}\right)^2 + \beta \left(\frac{\sigma_{12}}{S_c}\right)^2 - 1 \begin{cases} \geq 0 \text{ failed} \\ \leq 0 \text{ elastic} \end{cases} \quad (1)$$

Upon failure $E_1 = E_2 = G_{12} = \nu_{12} = \nu_{21} = 0$

Compressive fiber mode:

$$\sigma_{11} < 0 \text{ then } e_c^2 = \left(\frac{\sigma_{11}}{X_c}\right)^2 - 1 \begin{cases} \geq 0 \text{ failed} \\ \leq 0 \text{ elastic} \end{cases} \quad (2)$$

Upon failure $E_1 = \nu_{12} = \nu_{21} = 0$

Tensile matrix mode:

$$\sigma_{22} > 0 \text{ then } e_m^2 = \left(\frac{\sigma_{22}}{Y_t}\right)^2 + \left(\frac{\sigma_{12}}{S_c}\right)^2 - 1 \begin{cases} \geq 0 \text{ failed} \\ \leq 0 \text{ elastic} \end{cases} \quad (3)$$

Upon failure $E_2 = \nu_{21} = 0 \rightarrow G_{12} = 0$

Compressive matrix mode:

$$\sigma_{22} < 0 \text{ then } e_d^2 = \left(\frac{\sigma_{22}}{2S_c}\right)^2 + \left[\left(\frac{Y_c}{2S_c}\right)^2 - 1\right] \frac{\sigma_{22}}{Y_c} + \left(\frac{\sigma_{12}}{2S_c}\right)^2 - 1 \begin{cases} \geq 0 \text{ failed} \\ \leq 0 \text{ elastic} \end{cases} \quad (4)$$

Upon failure $E_2 = \nu_{21} = 0 \rightarrow G_{12} = 0$.

Parameter β , allows the introduction of the effect of the shear into the failure modes of the fibres. If β is equal to 1, the Hashin criteria would be implemented while if β is defined as 0 the maximum stress criteria would be used.

The material is considered to be failed and thus the indicated elastic modulus are subjected to degradation or it is considered to be completely unable to bear loading. The degree of property loss is strongly dependent upon the failure mechanisms and localized to the damaged elements.

A possible way to set the behaviour of the material after failure is using SLIMx parameters. They act on the residual strength of the element as follows: $\sigma_{residual} = SLIMx * \{Xt, Xc, Yt, Yc, Sc\}$

Two other parameters can be used to define the post damage behaviour:

FBRT defines the residual tensile fiber strength after compressive matrix failure

$$XT_{residual} = XT * FBRT$$

YCFAC defines the residual compressive fiber strength after compressive fiber failure

$$XC_{residual} = YC * YCFAC$$

Even if the material has failed, the element is still present. The element is deleted only after the tensile fibre mode failure. In order to cancel the elements some different parameters can be used:

If *DFAILT*—maximum strain for fiber tension—is zero, failure occurs if the Chang/Chang failure criterion is satisfied in the tensile fiber mode.

If *DFAILT* is greater than zero, failure occurs if the tensile fiber strain is greater than *DFAILT* or less than *DFAILC*. Other *DFAILx* parameters might be used to define deletion for the other failure modes. In Figure 7 the difference between the results obtained using *DFAILx* with Chang-Chang criteria is shown.



Figure 7. Chang-Chang Failure Criteria.

If EFS is greater than zero, failure occurs if the effective strain is greater than EFS , calculated as:

$$EFS = \sqrt{\frac{4}{3}(\epsilon_{11}^2 + \epsilon_{11}\epsilon_{22} + \epsilon_{11}^2 + \epsilon_{12})} \quad (5)$$

If $TFAIL$ is greater than zero, the element deletion depends on the time step as follows:
 $0 \leq TFAIL \leq 0.1$:

element is deleted when its time step is smaller than $TFAIL$, $TFAIL \geq 0.1$,
 element is deleted when

$$\frac{\text{current time step}}{\text{original time step}} < TFAIL \quad (6)$$

The minimum time step is defined by the highest distorted element. The parameters listed above are useful not only because they are necessary for deleting the elements but also because it is possible to tune the post damage behaviour. It was noticed that the contact between plies is a critical aspect regarding composite modelling since inter-laminar behaviour is complex to model and it plays a fundamental role in impact events.

3. Tail Design

The design of a breaking path begins with the analysis of the impact scenario, paying attention to the geometric shape, materials, and their speed envelopes. The tailgate has a square shape considered planar to a first approximation. This is useful to observe the stress distribution between the impact point and the support, and for this purpose, several simulations were performed varying the material, geometry and configuration. The numerical finite element simulations were performed using the commercial code LS/Dyna.

The tailgate presents dimensions of 696×696 mm, while the missile presents a radius of 95 mm and the relative distance between the panel curvature and the end of the rocket is 94 mm. The missile is supposed to have a spherical nose and an initial acceleration of about 15 g (150 m/s^2), typical of its category.

The requirements for the structural sizing are:

- Max weight 3.5 kg;
- The “Wave-load” is a distributed load of 0.6 bar;
- Failure for internal over-pressure of 1.5 bar;
- Failure for a force of 2500 N in the sphere center.

The missile ejection must be guaranteed without interference and any complications defining a controlled rupture of the hatch with no fragment along the missile exit direction. The debris should not be very large and should fall into a restricted area around the canister at low speed. The launch of the missile must be a safe operation for the ship and the crew on board and its reliability must be ensured throughout its operational life. Requirement-wise the structure has the task of protecting the missile, which will be in the canister a long time before its launch, against external agents.

The launching system operates in a humid environment rich in saltiness, and it is important to choose suitable materials. Moreover, the tailgate has the task of electromag-

netically shielding the missile from external threats, so it is covered with shielding paint to exploit the properties of the carbon-resin material.

The functional requirements must provide:

- Safe ejection.
- Correct fragmentation;
- No damage on the missile nose;
- A waterproof enclosure;
- Electromagnetic shielding.

The sphere strikes the plate at a velocity of 5.3 m/s^2 after 0.03535 s . To reduce the computational cost, the sphere has been placed at 10 mm with an initial velocity of 5.025 m/s . After studying the isotropic material behaviour and its stress distribution path, it is necessary to introduce the composite material to satisfy the lightness requirement. For the present work a carbon/epoxy laminate was chosen.

Initially, the analysis of a planar hatch with four petals and cruciform carvings was considered, as shown in Figure 8a, but to meet the design requirements, the concept of asymmetric impact must be introduced, as illustrated in Figure 8b. The latest missile configurations have a high nose, so the contact between the tailgate and the missile tip is not centred, which could compromise fragmentation and does not ensure safe ejection. For the simulation, it was considered that the contact is at the 66.5% of one edge while on the other side it is symmetric. In this case the lower petal, the largest one, is divided into two smaller triangular petals by introducing a carving along the height of the triangle, as shown in Figure 8c.

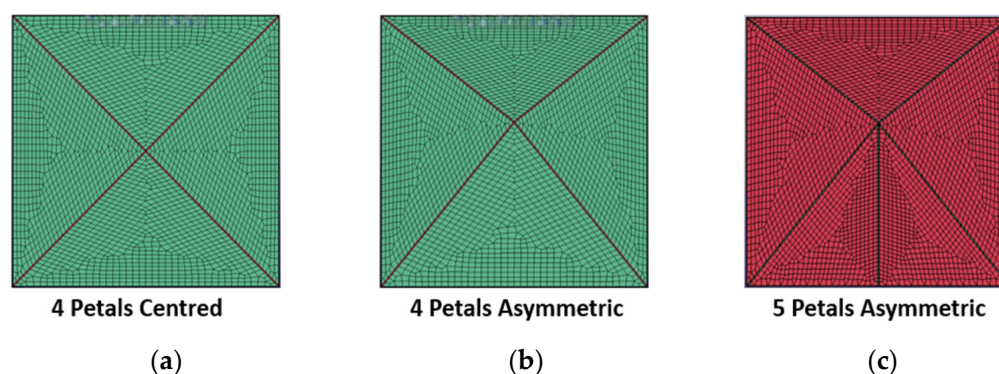


Figure 8. Planar tailgate configuration: (a) 4 petals centred, (b) 4 petals asymmetric, (c) 5 petals asymmetric.

Along the diagonal were introduced areas with only epoxy resin E-862 (carvings) of 2 mm that can help the fracture onset and the fragmentation of the square plate in 4 smaller triangular shape plates, the Table 2. Carvings become useful in driving the stress along the diagonals and this is important to define the fracture path. Afterwards, carvings were modelled along the sides of the square to ensure the correct fragmentation of the tailgate.

Table 2. Material characteristics of Epoxy-862.

Density	0.98 g/cm^3
Young's Modulus	8 GPa
Poisson ratio	0.3
Yield stress	60 MPa
Tangent modulus	2.34 GPa
Plastic strain at failure	3%

For the epoxy resin, we used the material sheet MAT_024_PIECEWISE_LINEAR_PLASTICITY, considering the curve shear-strain and stress-strain in Figures 9 and 10.

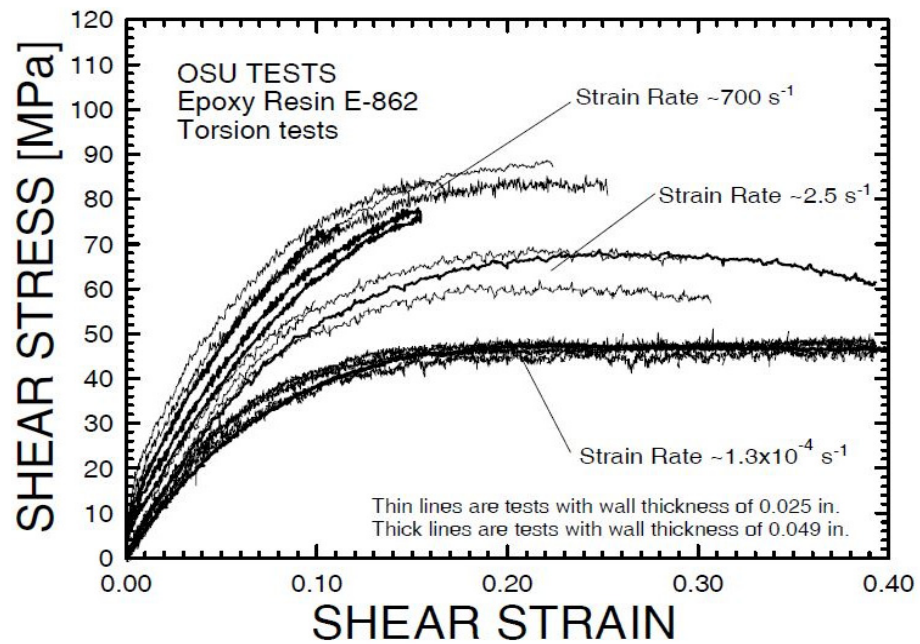


Figure 9. Shear stress-strain curve of Epoxy resin E-862.

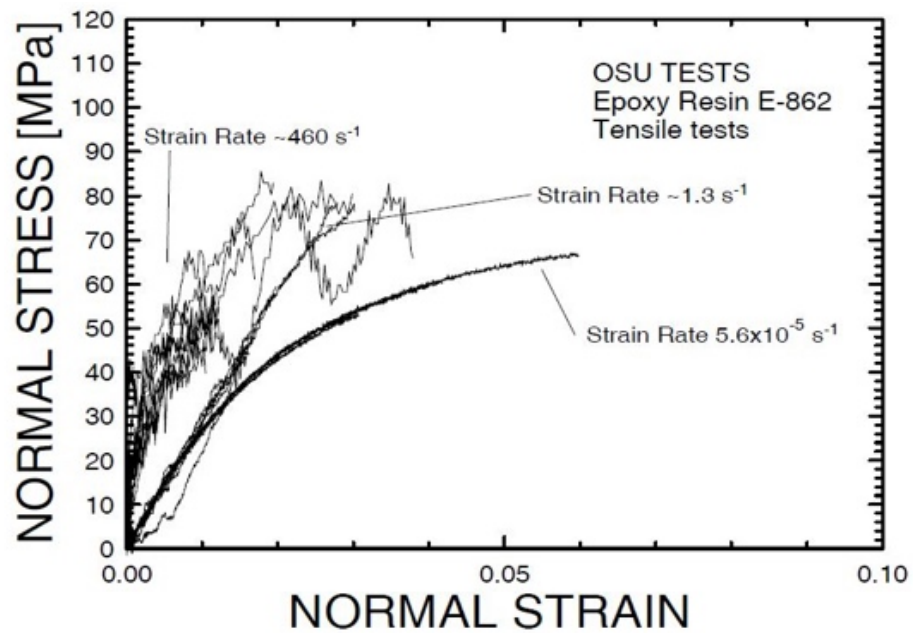


Figure 10. Normal stress-strain curve of Epoxy resin E-862.

The values of unidirectional E-8962 are reported in the Table 3.

In all investigated configurations the effective stress distribution of a square plate in composite material with diagonal carvings during impact was replicated, as shown in Figure 11. The effective stress is based on the equivalent stress concept derived from energy principles and is expressed in terms of a single three-variable criterion including the contribution of stress in the fiber direction.

The areas with only resin start in the point of contact and continue until the corner. The contact is closer to the upper edge, so due to the constraint condition the stress propagation path has a fast track in this direction. As a result, it needed to reduce the dimensions of the upper petal because of an incomplete fragmentation, and this represented an obstacle for the missile ejection because the debris were too large. To face this issue the bottom petal, which is the bigger, is divided in two smaller triangular petals introducing a carving

along the height of the triangle. This represents another fast track for stress propagation because the carving is directly on traction from the contact start. In addition, the new smaller bottom petals have lower flexural stiffness because the interlocking area is half while the arm is the same.

Table 3. Material properties of Carbon fiber E-862 unidirectional tape.

Property	Symbol	LS-DYNA Parameter	Value
density	ρ	RO	1.5 g/cm ³
Modulus in 1-direction	E_1	EA	134 GPa
Modulus in 2-direction	E_2	EB	7 GPa
Shear modulus	G_{12}	GAB	4.2 GPa
Major Poisson’s ratio	ν_{12}	-	0.2
Minor Poisson’s ratio	ν_{21}	PRAB	0.1
Strength in 1-direction, tension	F_1^{tu}	XT	1270
Strength in 2-direction, tension	F_2^{tu}	YT	42 MPa
Strength in 1-direction, compression	F_1^{cu}	XC	1130 MPa
Strength in 2-direction, compression	F_2^{cu}	YC	141 MPa
Shear strength	F_{12}^{su}	SC	63 MPa

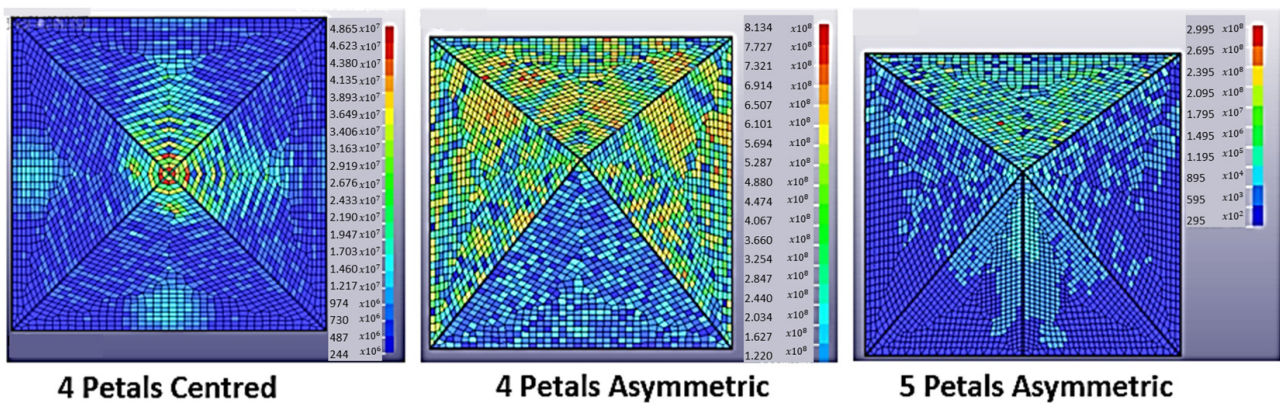


Figure 11. Planar tailgates: Stress Distribution.

The stresses are very high in both symmetric and asymmetric impact, but the introduction of a carvings area can mitigate the peak of stress by having a progressive failure, as reported in Figure 12.

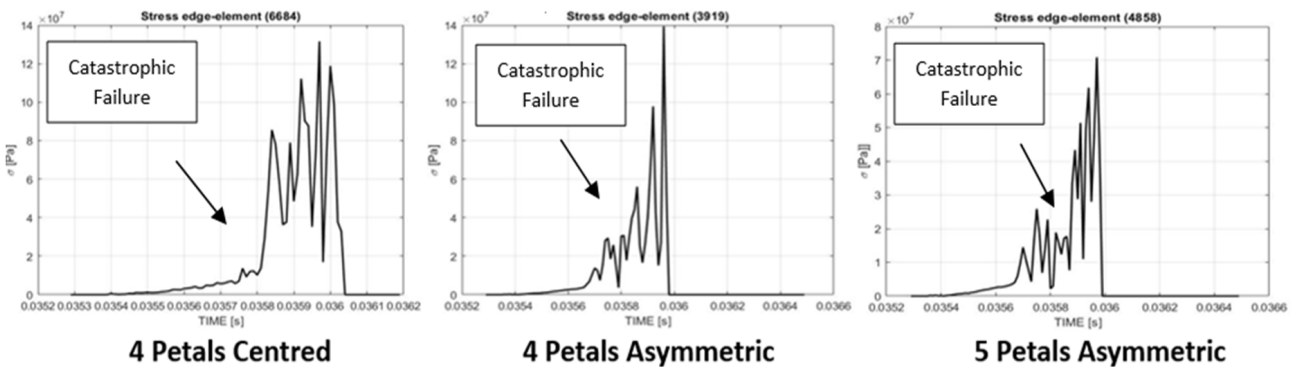


Figure 12. Planar Tailgates: stress distribution.

The numerical simulations underlined how the asymmetric configuration with five petals achieves a good breaking path, but the stresses are too high, and the petals detach at the same time, hindering launch, as shown in Figure 13.

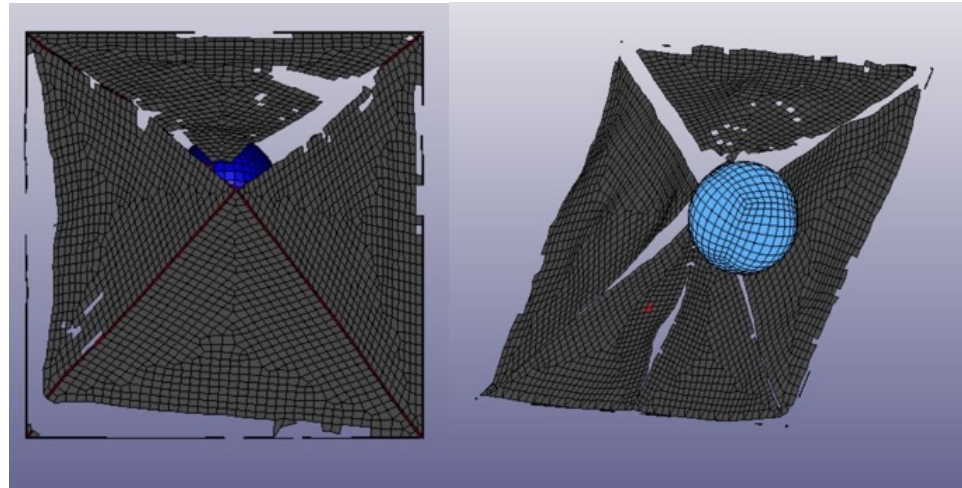


Figure 13. Four Petals Asymmetric VS Five Petals Asymmetric: Impact Simulation.

An introduction of an angled impact allows for the exploiting of the constant acceleration profile and to reach a higher rotational speed of petals around the sides during the impact and therefore a greater kinetic energy. Curved structures can absorb large amounts of energy due to their shape and ability to deform and allow large displacements before breakage. Two other configurations were investigated: a multifaced pyramid and a pavilion dome to improve the fracture behaviour and the load distribution, as shown in Figure 14.

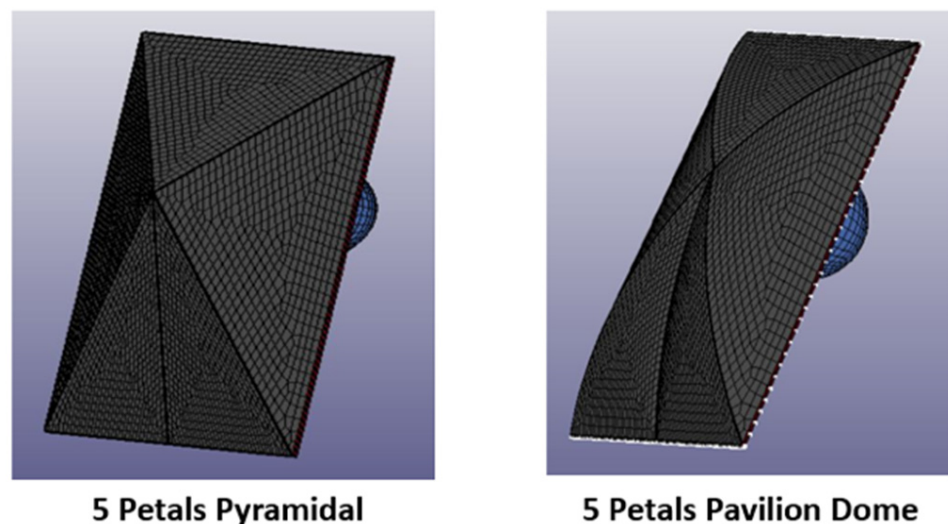


Figure 14. Pyramidal and Pavilion Dome Tailgate Configuration.

The impact angle influences the contact force because the contact is more localized; nevertheless, the impact duration increases because not every part of the structure is involved in the impact event from the beginning. For a pyramidal multifaced configuration, the highly concentrated load produces an indentation on the petal that can damage the missile tip where sensitive and delicate electrical systems are integrated. The simulation shows that the fragmentation in five petals occurs and that the petals rotate around the tailgate's supports, ensuring a clean ejection. The problem regarding the initial contact force may be mitigated by the introduction of curvature, which will be investigated in the dome model simulation.

Curved structures have excellent characteristics when subjected to pressure load because bending loads were converted in tensile loads and the stress distribution is almost uniform. The vault is engineered through 5 arcs of circumference, lying on planes orthogonal to the base-plane, four from the square’s corner and one on the bigger petals from the vertex to the middle of the base-edge. The four arcs from the corner to the vertex have a radius of 1 m, while the other arc has a bigger radius of 1.5 m. This architecture anticipates the contact between the tailgate and the sphere.

The fracture begins in the dome vertex by tensile stress in carving on the smaller pavilion side and then the whole structure is involved in bending loads until the complete fragmentation, as shown in Figure 15.

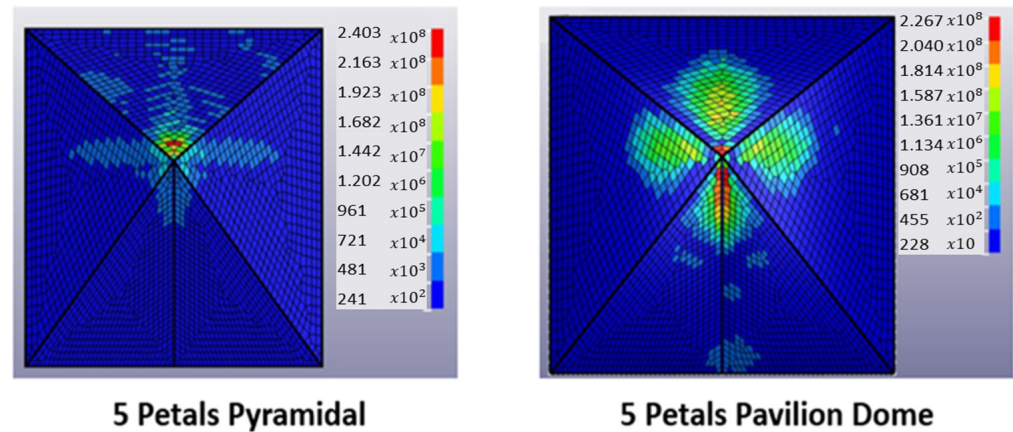


Figure 15. Pyramidal and Pavilion Dome Tailgate Configuration: Stress Distribution.

The contact area is larger than the previous ones. Even though the two contact-surfaces have a different radius, the tailgate’s surface adapts to the sphere’s surface thanks to the deformation.

4. Results

The five simulation models consist of three shape configurations (planar, pyramidal, dome) respecting the overall dimensions and the weight limitations. The best solution for the static requirement is the pavilion dome, as reported in the Figure 16, because in addition to supporting the static “wave load”, it allows for the management of the breakage by pressure load, but this aspect must be studied further.

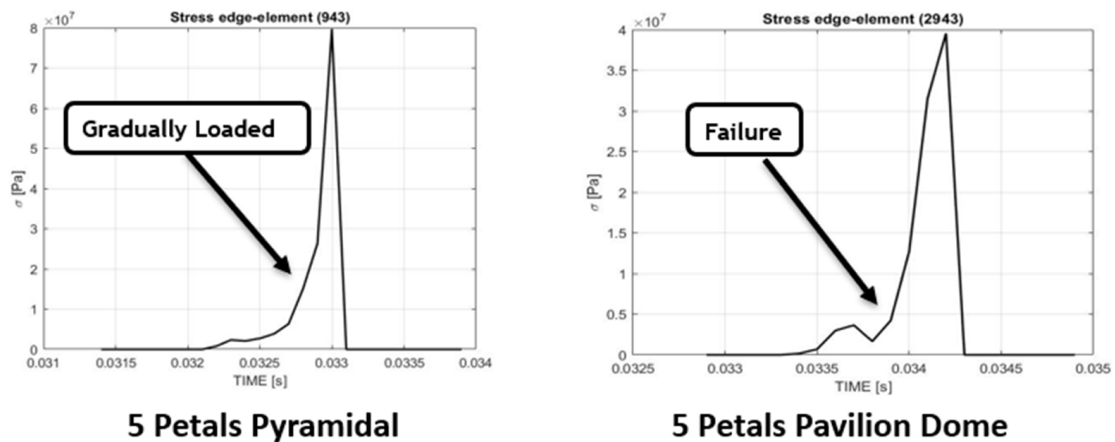


Figure 16. Pyramidal and Pavilion Dome Tailgate configuration: Stress evaluation.

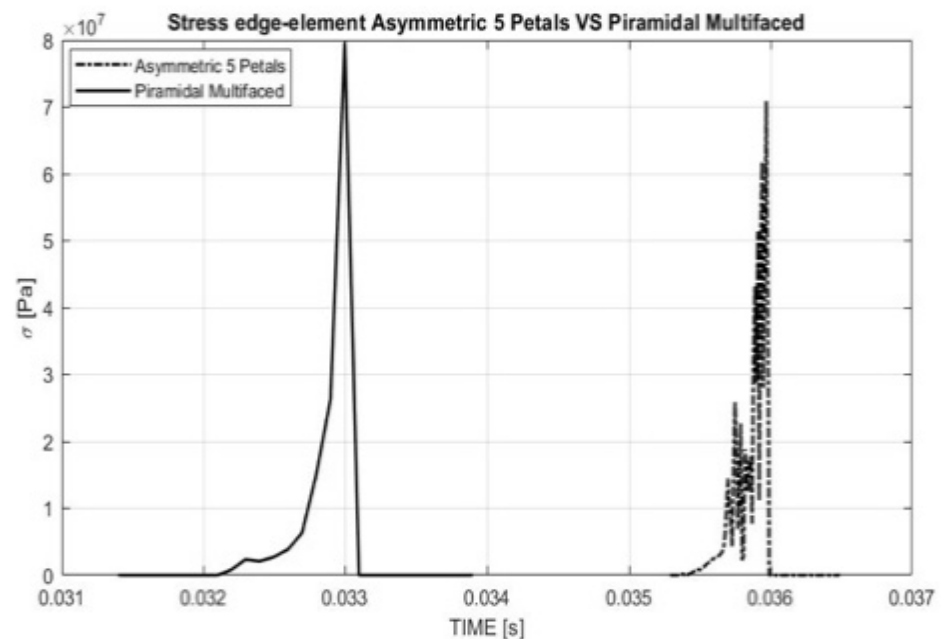
Table 4 summarizes all of the results collected:

Table 4. Numerical results.

Configuration	Time [s]	Breakage Time [s]	Von Mises Stress [MPa]	Weight [kg]
Planar 4 Petals Centred	0.035	7×10^{-4}	131	2.02
Planar 4 Petals Asymmetric	0.035	6×10^{-4}	139	2.10
Planar 5 Petals Asymmetric	0.035	6×10^{-4}	70	2.08
Planar 4 Petals Asymmetric	0.035	6×10^{-4}	139	2.10
Pyramidal Multifaced	0.032	1.4×10^{-3}	79	2.80
Pavilion Dome	0.033	1×10^{-3}	39	3.17

Planar configuration is lighter, but it has a faster and a more sudden breakage, and this can lead to the uncorking of the tailgate or damaging the missile tip. The petals fail due to the in-plane bending stresses and shear stresses. The stresses are very high in both symmetric and asymmetric impact, but introducing carvings can mitigate the peak of stress by having a progressive failure.

The introduction of an impact angle due to multifaced pyramidal and dome structures helps to increase the duration of impact and to give rotational speed around the edges to the petals, as shown in Figure 17. The structures exhibit a smoother behaviour, but for the pyramidal one the contact force is more concentrated, causing indentations, while the pavilion dome exhibits a softer and a more gradual contact.

**Figure 17.** Planar VS Pyramidal Multifaced Tailgate: Stress evaluation.

Thanks to the curvature design optimization, the pavilion dome structure shows low stress levels and longer times for breakage, as shown in Figure 18. The tailgate subjected to impact has a more gradual breakage and, as seen in the following figure, the Von Mises stress in an edge element after an initial growth goes down until the whole structure is involved and the element fails for tensile load.

The pavilion dome structure was more suitable to reach the goal because it resists better under pressure load and allows the designer to manage the carving curvature to optimize the structure fragmentation, as shown in Figure 19.

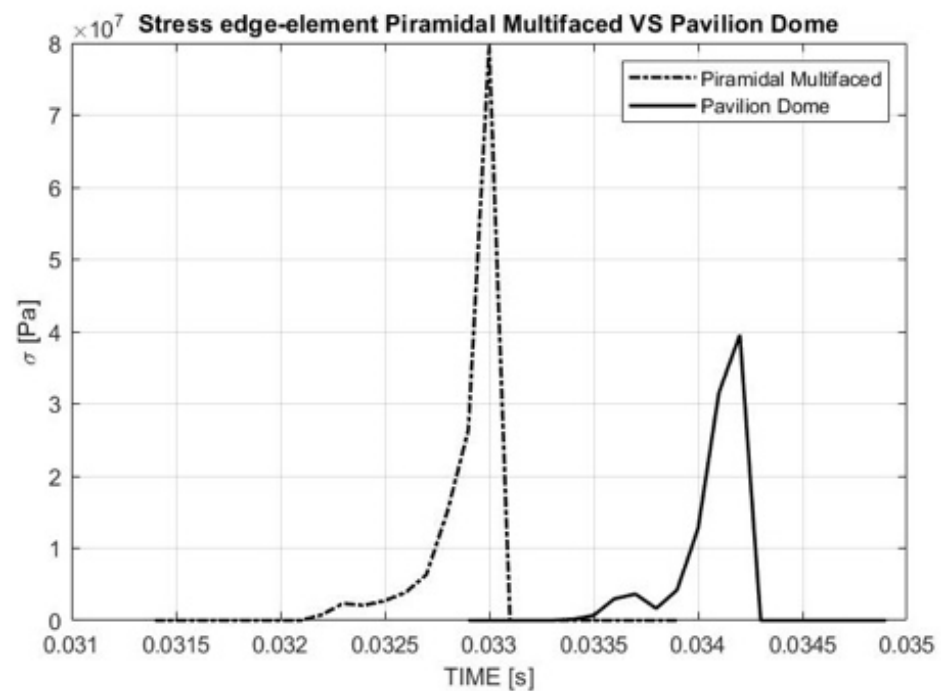


Figure 18. Pyramidal Multifaced VS Pavilion Dome Tailgate: Stress evaluation.

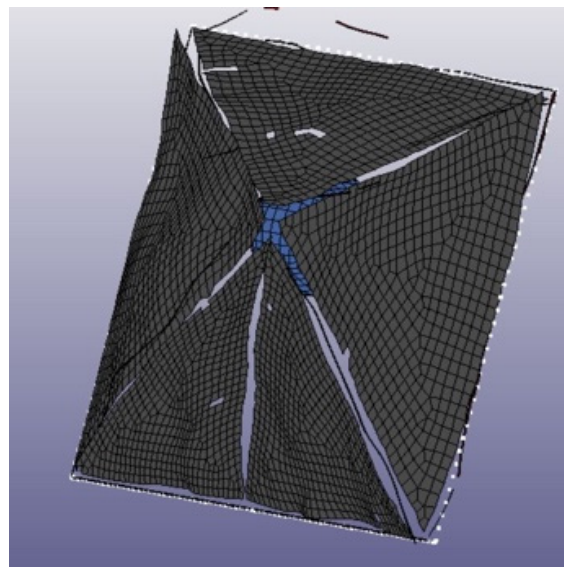


Figure 19. Simulation of Dome Tailgate's fragmentation after impact.

5. Conclusions

The analysis of the mechanical behavior of the frangible composite canister has been proposed. The frangibility and controlled separation process was simulated using the FE model. The numerical deformation of the canister and the breakdown pressure of the frangible plate were determined for five different geometries using three shape configurations (planar, pyramidal, dome).

The study showed that the pavilion dome structure shows low stress levels and a longer time for breakage, related to the planar configuration, which is lighter, but also has a faster and a more sudden breakage, and this can lead to the uncorking of the tailgate or damaging the missile tip. This solution invites the petals to fail to the in-plane bending stresses and shear stresses and the mechanical behavior of the breakable canister and the failure criteria in predicting failure are reasonable and acceptable for design and optimization.

The main achievement of this research was the collection of results, obtained by both simplified realistic and full-scale FE model analysis, to define a design “rule of thumb” assessment about the missile ejection problem. It has permitted the tracing of the guidelines to perform the design process of a controlled rupture structure during impact.

Author Contributions: Conceptualization, M.G. and F.M.; methodology, M.C. and R.M.; software, M.G. and A.S.; validation, M.G., A.S. and F.M.; formal analysis, M.G. and F.M.; investigation, M.C., R.M.; resources, M.C.; data curation, M.G., A.S. and F.M.; writing—original draft preparation, A.S.; writing—review and editing, M.G.; visualization, A.S., R.M., M.G. and F.M.; supervision, M.G. and F.M.; project administration, M.G. and F.M.; funding acquisition, M.G. and F.M. All authors have read and agreed to the published version of the manuscript.

Funding: This research received no external funding.

Institutional Review Board Statement: The study did not require ethical approval.

Informed Consent Statement: Not applicable.

Data Availability Statement: Not applicable.

Conflicts of Interest: The authors declare no conflict of interest.

References

1. Copeland, R.L.; Greene, R.F. Protective Cover for a Missile nose Cone. US Patent 3,970,006, 20 July 1976. Available online: <https://patents.google.com/patent/US3970006A/en> (accessed on 1 January 2020).
2. Boeglin, P.H. Plate Glass Window Fitted with an Explosion-Cutting Device. U.S. Patent 4,333,381, 6 April 1982. Available online: <https://patents.google.com/patent/CA1121324A/en> (accessed on 1 January 2020).
3. Doane, W.J. Frangible Fly through Diaphragm for Missile Launch Canister. U.S. Patent 4,498,368, 12 February 1985.
4. Choi, W.; Jung, S. Launch Performance Degradation of the Rupture-Type Missile Canister. *Appl. Sci.* **2019**, *9*, 1290. [[CrossRef](#)]
5. Cai, D.; Zhou, G.; Qian, Y.; Silberschmidt, V.V. Failure analysis of a frangible composite cover: A transient-dynamics study. *J. Compos. Mater.* **2017**, *51*, 2607–2617. [[CrossRef](#)]
6. Guida, M. Validity and applicability of the scaling effects for the low velocity impact on composite plates. *Materials* **2021**, *14*, 5884. [[CrossRef](#)] [[PubMed](#)]
7. Wu, J.H.; Wang, W.T.; Kam, T.Y. Failure analysis of a frangible laminated composite canister cover. *Proc. Inst. Mech. Eng.* **1999**, *213*, 187–195. [[CrossRef](#)]
8. Chang, F.; Chang, K. A progressive damage model for laminated composites containing stress concentrations. *J. Compos. Mater.* **1987**, *21*, 834–855. [[CrossRef](#)]
9. Zhang, C. Computational and experimental investigation of progressive damage accumulation in I-plate composite structure. *J. Phys. Conf. Ser.* **2020**, *1676*, 012062.
10. Davies, G.A.O.; Hitchings, D.; Wang, J. Prediction of threshold impact energy for onset of delamination in quasi-isotropic carbon/epoxy composite laminates under low-velocity impact. *Compos. Sci. Technol.* **2000**, *60*, 1–7. [[CrossRef](#)]
11. Ghasemnejad, H.; Hadavinia, H.; Aboutorabi, A. Effect of delamination failure in crashworthiness analysis of hybrid composite box structures. *Mater. Des.* **2010**, *31*, 1105–1116. [[CrossRef](#)]
12. Tsartsaris, N.; Dolce, F.; Polimeno, U.; Meo, M.; Guida, M.; Marulo, F. Low velocity impact behavior of fibre metal laminates. *J. Compos. Mater.* **2011**, *45*, 803–814. [[CrossRef](#)]
13. Marulo, F.; Guida, M.; Maio, L.; Ricci, F. Numerical simulations and experimental experiences of impact on composite structures. In *Dynamic Response and Failure of Composite Materials*; Lopresto, V., Langella, A., Abrate, S., Eds.; Springer: Dordrecht, The Netherlands, 2017; ISBN 9780081008874.
14. Wade, B.; Feraboli, P.; Rassaian, M. *Ls-Dyna MAT54 for Simulating Composite Crash Energy Absorption*; JAMS Workshop Technical Review: San Diego, CA, USA, 2011.
15. Guida, M.; Marulo, F.; Belkhef, F.Z.; Russo, P. A review of the bird impact process and validation of the SPH impact model for aircraft structure. *Prog. Aerosp. Sci.* **2022**, *129*, 100787. [[CrossRef](#)]
16. Guida, M.; Marulo, F.; Meo, M.; Riccio, M. Analysis of Bird Impact on a Composite Tailplane Leading Edge. *Appl. Compos. Mater.* **2008**, *15*, 241–257. [[CrossRef](#)]